ANALYSIS OF THE SPATIAL VARIABILITY OF SNOW COVER DEPLETION IN AN ALPINE WATERSHED, TOKOPAH BASIN, SIERRA NEVADA, CALIFORNIA, U.S.A.

Noah P. Molotch[1], Thomas H. Painter[2], Michael T. Colee[2], Charles W. Rosenthal[3], Jeff Dozier[3], Roger C. Bales[1]

ABSTRACT

In this study we quantified the spatial and temporal depletion of snow covered area (SCA) in order to obtain estimates of peak snow water equivalence (SWE) in the 19.1 km^2 Tokopah Basin. We sought to answer the following questions: How do we improve the use of snow cover depletion curves by incorporating additional data and spatial analysis? How can we use snow cover depletion curves to estimate peak SWE earlier in the snowmelt season and continue to have leverage to update our estimates throughout the ablation season? What meteorological fields or combination of meteorological fields yield the most leverage in updating SWE estimates? In order to quantify snow cover depletion at different elevations and under different topographic environments, we analyzed snow cover depletion patterns in different elevation zones and in sub-basins of varying topographic heterogeneighty. We used 30m remotely sensed SCA data, hourly meteorological data, ground-based surveys of SWE and a 30m digital elevation model (DEM). We generated depletion curves of SCA using two methods of varying complexity: SCA versus modeled accumulated degree-days and SCA versus modeled net radiation. We found that SWE over the basin during the April, May and June snow surveys was 995mm, 701mm and 283mm respectively. Degree-day accumulation produced decreases in SCA at lower elevations (<2823m) before SCA decreased at higher elevations (>3222m). Degree-day depletion curves did not represent observed temporal variability in SWE during the ablation season. Depletion curves using net radiation as the response variable proved to better represent temporal SWE variability. We found that incremental decreases in SCA at higher elevations (>3222m) resulted in a greater decrease of SWE than the corresponding SWE decrease at lower elevations (<2823m).

INTRODUCTION

Snow water equivalence stored in the Sierra Nevada of California is an essential source of water for California agriculture. It is estimated that snow from the Sierra Nevada provides three fourths of the water supply for the states agriculture (Rosenthal, 1996). Currently, operational streamflow forecasts are based on empirical snowmelt runoff models that may not perform well under extreme or unusual climatic seasons; therefore, current research efforts are aimed at estimating stream discharge using distributed physically based snowmelt runoff models. These models will require estimates of distributed SWE as an input for the beginning of the model run at peak SWE accumulation. Rango and Martinec (1982) showed that basin-wide SWE can be calculated using snow cover depletion curves of SCA using accumulated degree-days as the response variable. This approach incorporated SCA depletion processes into estimates of SWE but the estimates are still empirical estimates of SWE. Cline et al. (1998) showed that snow cover depletion data from remotely sensed imagery can be used in conjunction with estimates of energy balance variables to back-calculate SWE on a pixel-by-pixel basis throughout the melt season. In this research we attempt to add to the aforementioned studies by comparing depletion curves of SCA using modeled accumulated degree-days and modeled net radiation as the response variables. The goal of this research is to incorporate process-oriented information into empirical SWE estimates while minimizing computational demand. We conducted this research in the heavily studied Tokopah Basin of the Sierra Nevada, located in Sequoia National Park (figure 1). The Tokopah Basin is a 1910 ha alpine basin located at approximately 36°36'N, 118°40W. The altitude of the basin ranges from 2622 to 3487m. Granite bedrock covers most of the basin and forest cover is restricted to small areas in the valley floor. Tonnessen (1991) provides a detailed description of the Emerald Lake sub-basin. The precipitation in the basin is dominated by snowfall from frontal storms originating from the Pacific Ocean. Summer season precipitation inputs are low but occur in the form of rainfall from convective storms.

Paper presented at the 69th Annual Meeting of the Western Snow Conference, 2001.

[1] Department of Hydrology and Water Resources, University of Arizona
[2] Institute for Computational Earth System Science, University of California, Santa Barbara
[3] Donald Bren School of Environmental Science and Management, University of California, Santa Barbara

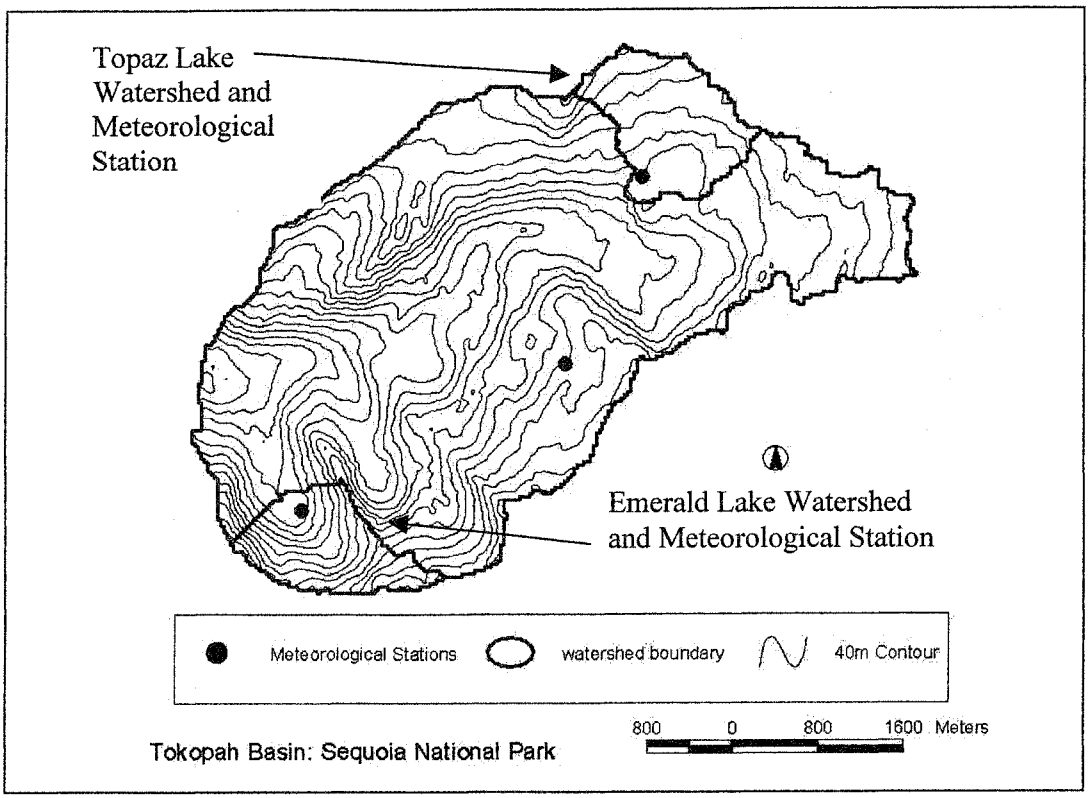

Fig. 1: Tokopah Basin boundary with Emerald Lake and Topaz Lake Sub-basin boundaries. Locations of meteorological stations are also shown.

METHODS

Using a combination of ARC/GRID, an atmospheric radiative transfer model, a one dimensional snowmelt model, a 30m DEM and meteorological data from three meteorological stations (figure 1), we modeled accumulated degree-days (ADD) and accumulated net radiation (ANR) at 30m-spatial resolution across eight elevation bands at hourly temporal resolution from day of year (DOY) 96 – 176, 1997. Figure 2 shows a conceptual flow diagram of the modeling procedure. We then plotted the average ADD and ANR of each elevation band against the average SCA over the elevation band on each day for which we had SCA data (see figure 2). Using ground-based observations of SWE we qualitatively evaluated the ability of the two different approaches to represent the evolution of SWE during the snowmelt season.

Snow Covered Area Surfaces

We used satellite imagery from the Landsat Thematic Mapper (TM) on April 6, April 22, May 8, June 6, and June 25, 1997 to construct SCA images across the basin using the algorithm of Rosenthal and Dozier (1996). Imagery from the Airborne Visible and Infrared Imaging Spectrometer (AVIRIS) was also used to obtain SCA data on May 8 and May 21, 1997. SCA surfaces at 30m spatial resolution were created across the basin and converted to a scale of 0 – 1 for use in the equations below.

Temperature Surfaces

Air temperature surfaces were modeled by deriving an environmental lapse rate in the basin for each hour of the model run using air temperature data from three meteorological stations. We then applied the lapse rate to every pixel in the basin using the DEM [Colee, 2000; Daly et al., 1994; Raskin et al., 1997; Thornton et al., 1997; Willmott and Matsu ura, 1995].

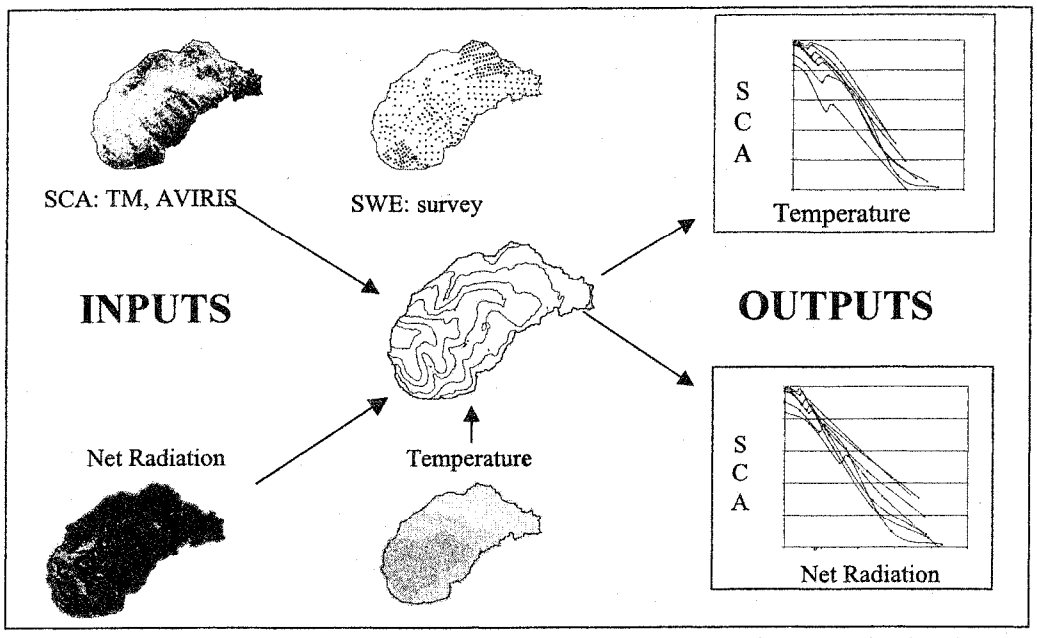

Figure 2: Flow diagram of model: clockwise from top left) Landsat Thematic Mapper (TM) and Airborne Visible and Infrared Imaging Spectrometer (AVIRIS) SCA data, ground based SWE data (used for validation), example depletion curves, air temperature surfaces derived from meteorological stations, net radiation surfaces derived from atmospheric radiative transfer model. Center: Elevation band delineation used to separate basin.

Net Radiation Surfaces

We modeled net radiation for each pixel in the basin using the following equation:

$$R_{net} = S_{net} + L_{in} - L_{out}$$

Where:
R_{net} = net radiation
S_{net} = net solar radiation
L_{in} = incoming longwave radiation
L_{out} = outgoing longwave radiation

In this model we assumed that the land cover of the basin was either snow or rock. In order to account for the different spectral and thermal properties of snow and rock we incorporated SCA data to give us the percentage of each pixel covered by snow or rock. The procedures used to model each variable in the above equation are described in the sub-headings below.

Net Solar Radiation

We calculated net solar radiation using the following equation:

$$S_{net} = [[S_{in} * (1 - a_{snow})] * SCA] + [[S_{in} * (1 - a_{rock})] * RCA]$$

Where:
S_{in} = incoming solar radiation
a_{snow} = snow albedo (assumed 0.78)
a_{rock} = granite albedo (assumed 0.36)
RCA = rock covered area (1 – SCA)

TOPORAD (Dozier, 1980; Dozier and Frew, 1990) was used to model incoming solar radiation at the Emerald Lake and Topaz Lake meteorological stations (figure 1). Using LOWTRAN7 (Dubayah, 1991; Kneizys et al., 1998), we calculated the atmospheric transmission parameters that caused TOPORAD to match the observed incoming solar radiation values at the two meteorological stations. This was done for 5 different atmospheric conditions ranging from clear sky to cloud cover. Using these atmospheric parameters, TOPORAD was then used to model the incoming solar radiation across the basin.

We used an assumed snow albedo of 0.78 and a granite albedo of 0.36, as determined from spectral measurements made in the field, the details of which are beyond the scope of this paper. Rock covered area (RCA) for each pixel was determined from the SCA images using the equation:

$$RCA = 1 - SCA$$

Incoming Longwave Radiation

We modeled incoming longwave radiation using a method similar to that of Colee (2000) and Cline et al. (1998a; 1998b). Using the interpolated temperature surfaces (as described above) and relative humidity surfaces (interpolated using the same method as the temperature surfaces) we applied the equations of Idso (1981) to the modeled relative humidity and temperature of each cell to compute the incoming longwave radiation. The RMSE over the modeling period was 34 W/m^2 at the Emerald Lake meteorological station and 40 W/m^2 at the Topaz Lake meteorological station.

Outgoing Longwave Radiation

Outgoing longwave radiation was calculated for each pixel using the following equation:

$$L_{out} = (\varepsilon_{snow} * \sigma * T_{snow}^4 * SCA) + (\varepsilon_{rock} * \sigma * T_{rock}^4 * RCA)$$

Where: L_{out} = outgoing longwave radiation
ε_{snow} = snow emissivity (0.98)
ε_{rock} = rock emissivity (0.85)
σ = Stephan-Boltzman Constant ($5.67 \times 10^{-8} W^{-2} K^{-4}$)
T_{snow} = snow surface temperature (K)
T_{rock} = rock surface temperature (K)

An assumed snow emissivity of 0.98 and an assumed granite emissivity of 0.85 (Lillisand and Kiefer) was used. We modeled snow surface temperature across the basin using a distributed version (Colee, 2000) of the one-dimensional snow surface temperature model, SNTHERM.89 (Jordan, 1991). The snow temperature model was initialized using snow temperature profiles recorded in the field in 7 snowpits across the basin (figure 4). We then interpolated these profiles across the basin using an exponential decay function with a 200m radius of influence.

Rock temperature was modeled using an empirically derived relationship between air temperature and rock temperature. We derived this equation using air and ground surface temperature sensors located at the Mammoth Mountain Energy Balance Station in the Sierra Nevada of California. Figure 3 shows the relationship between air and rock temperature from 07/01/01 to 09/15/01. We separated the day and night time temperatures and derived empirical equations for day and night temperatures separately. Then we applied the appropriate equation to each pixel within the basin throughout the model run.

Snow Surveys

We sampled snow depth during three different surveys lasting approximately one week each. Figure 4 shows the locations of the measurements. Depth measurements were made on a grid of approximately 240m across the Tokopah Basin and at 100m-grid resolution in the Emerald and Topaz Lake sub-basins. At each point we recorded the location using GPS and 3 corresponding depth measurements. We sampled these 3 depth measurements approximately 5m apart so that micro-topographical influences could be accounted for. We conducted the first survey on April 6^{th} – 12^{th} 1997, the second on May 8^{th} – 15^{th}, 1997 and the third on June 16^{th} – 18^{th} 1997. Density measurements were made using a Federal Sampler and snowpit data. The density and depth point coverages were interpolated using an Inverse Distance Weighting function in which the 12 nearest samples were used in the interpolation.

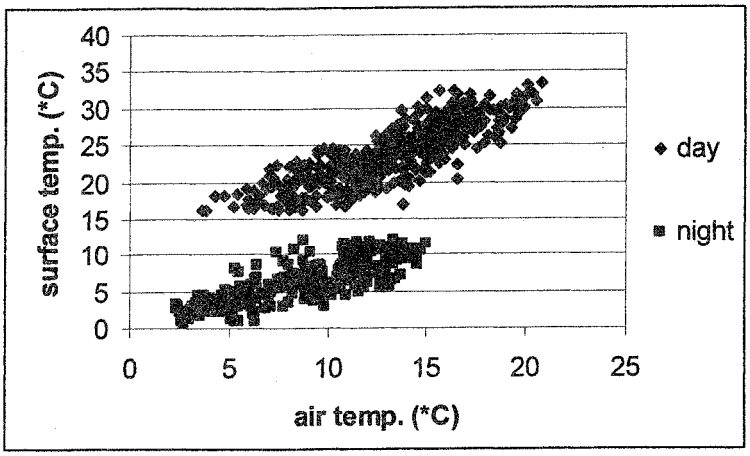

Figure 3: Relationship between surface and air temperature at Mammoth Mountain, California on 07/01/01 to 09/15/01.

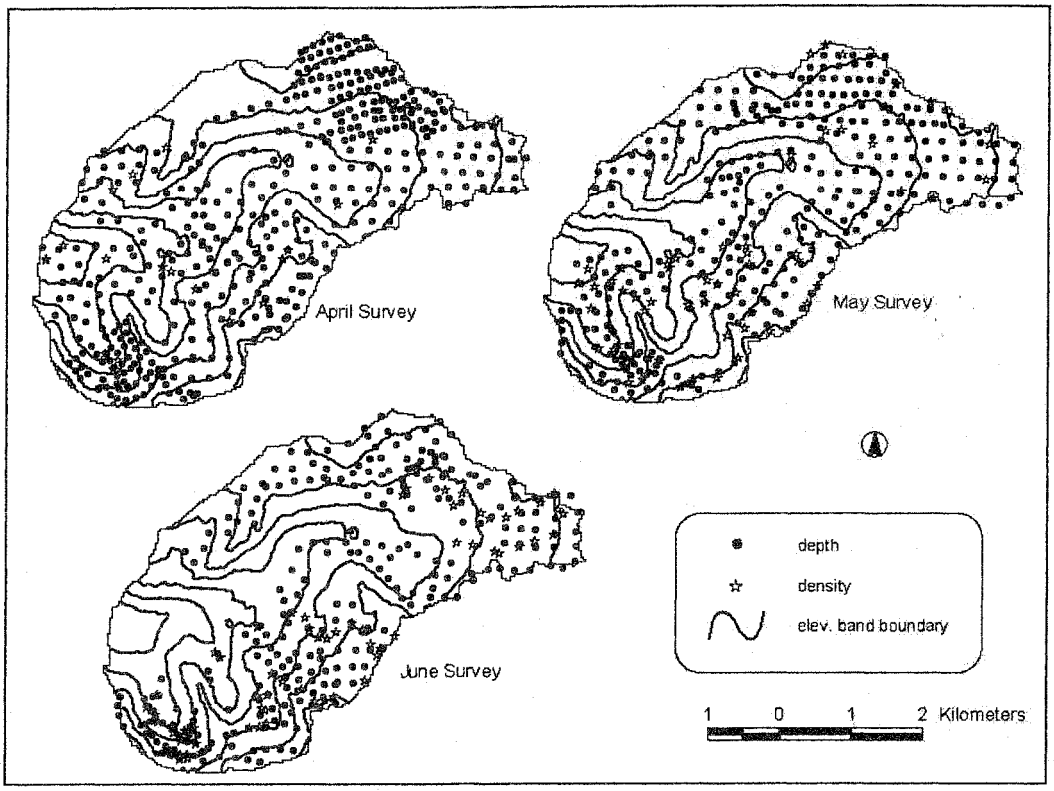

Figure 4: Snow depth and snow density data locations for the April, May and June 1997 snow surveys.

RESULTS AND DISCUSSION

Across the Tokopah basin SCA decreased more dramatically in the lower elevation bands (see figure 5). The curves in figure 5 are fairly well ordered with higher elevation bands at the top of the graphs and lower elevation bands at the bottom. The net radiation curves deviate in shape whereas the degree-day curves have similar slopes and shapes for all of the elevation bands. At the onset of the snowmelt season SCA did not decrease substantially with initial increases in ADD and ANR. This is likely due to snowmelt occurring in the vertical plane prior to the horizontal.

Figures 6 and 7 show similar curves for the Emerald and Topaz Lake Watersheds. The Topaz Lake Watershed is topographically homogeneous relative to the Emerald Lake Watershed and therefore the depletion curves at Topaz are uniform relative to Emerald.

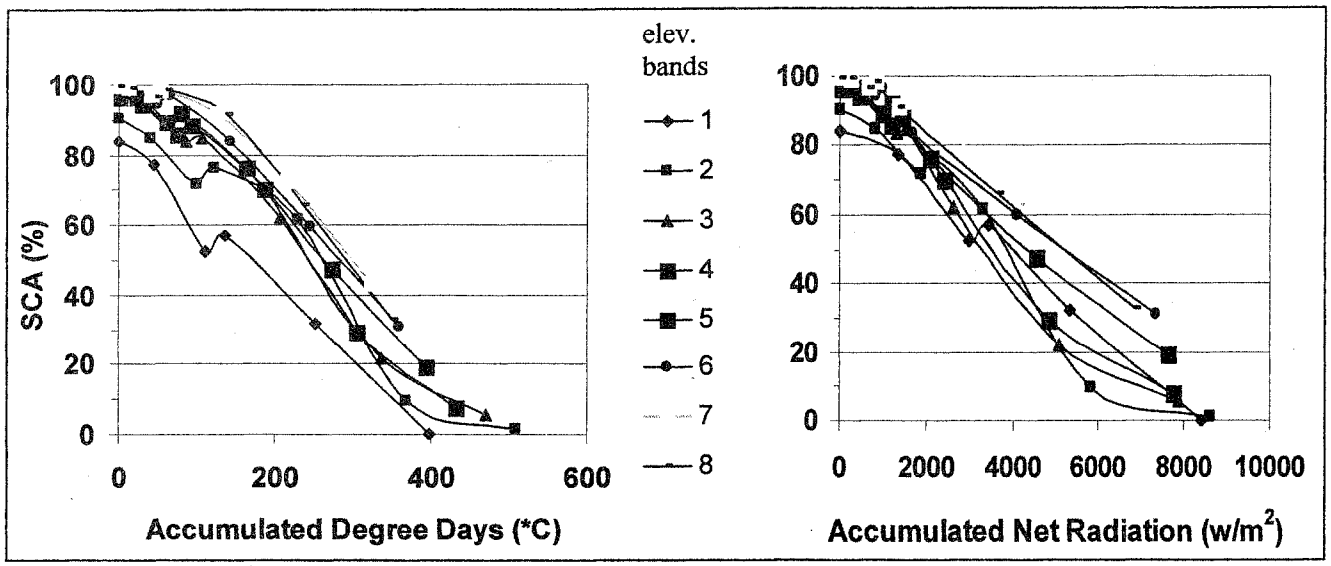

Figure 5: Accumulated net radiation and accumulated degree-day depletion curves for the Tokopah Basin. Elevation bands are numbered 1 – 8 from low (2622m) to high (3488m) elevation.

In the Emerald Lake Watershed the curves show a weak correlation with elevation, contradictory to what was seen across the Tokopah Basin. This is likely due to wind and avalanche redistribution of snow from higher to lower elevation zones. Additionally, SCA values in the higher elevations of Emerald are constrained by large rock outcroppings that are consistently snow free throughout the snowmelt season. When comparing the net radiation and degree-day curves it is apparent that there is little difference in the variability of the curves at Topaz. Given that snow cover is relatively homogeneous in Topaz it is intuitive that the net radiation and degree-day curves would be similar. At Emerald the two sets of curves show substantial variability from one another. Unlike the net radiation curves, the degree-day curves do not deviate as the snowmelt season progresses. This is due to the fact that the net radiation methodology accounts for exposed rock in calculating the magnitude of the response variable in each pixel. Conversely, the degree-day methodology does not account for any differences in the radiative emission of rock and snow. Given that exposed rock can emit a large amount of thermal radiation, decreases in SCA can be highly sensitive to nearby exposed rock. Thus the net radiation curves do a better job at representing SCA depletion in the Emerald Lake Watershed.

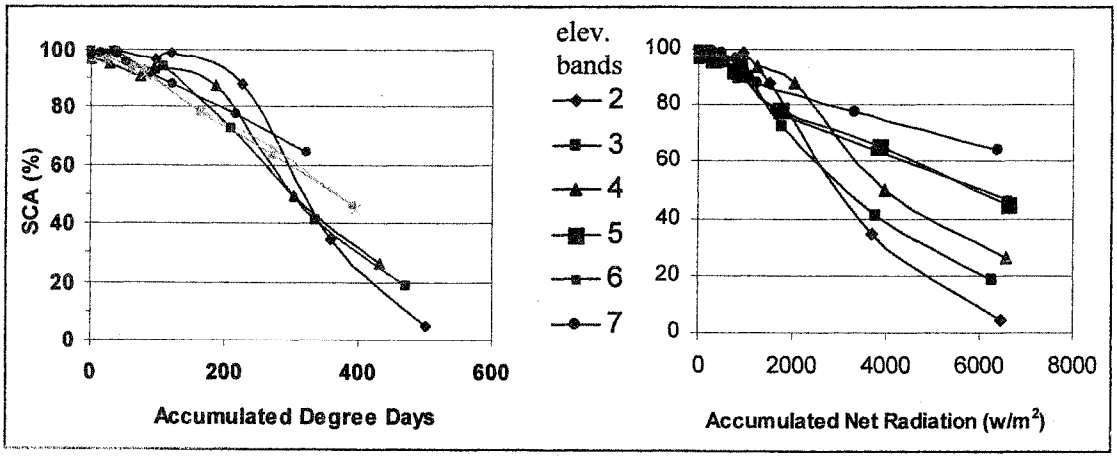

Figure 6: Degree-day and net radiation curves for the Emerald Lake Watershed.

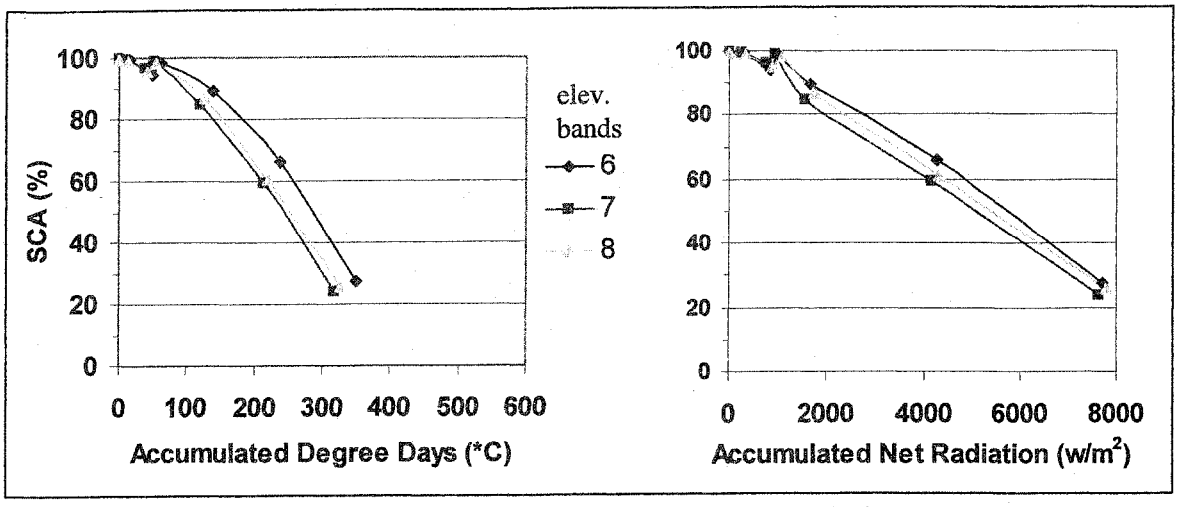

Figure 7: Degree-day and net radiation curves for the Topaz Lake Watershed

Decreases in SWE at the beginning of the snowmelt season did not result in the drastic decreases in SCA observed in the latter part of the snowmelt season (see figure 8). This was do to the fact that decreases in SWE at the beginning of the snowmelt season tended to deplete snow in the vertical direction, followed by decreases in SWE in the horizontal directions (i.e. decreases in SCA). Figure 8 illustrates this process, as the slopes of the first sections of the curves (going from left to right), are steeper at higher elevation. Decreases in SWE in the higher elevations did not result in decreases in SCA until later in the snowmelt season.

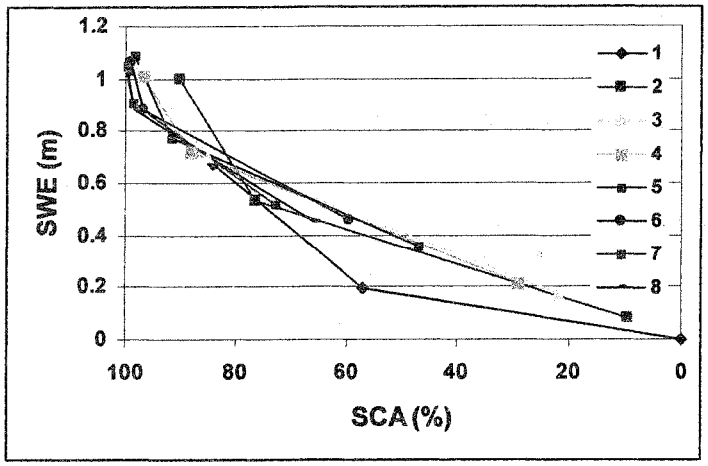

Figure 8: Relationship between SCA and SWE for the 8 elevation bands of the Tokopah Basin

CONCLUSION

Comparing elevation bands 3,5 and 7 illustrates the ability of the net radiation curves to represent snow cover depletion. As shown by the column chart in figure 9, SWE in elevation bands 3,5 and 7 is relatively similar at the beginning of the melt season but as the melt season progresses SWE begins to deviate substantially. The corresponding depletion curves show that changes in SWE can be best represented by the net radiation curves as evidenced by the deviation in the net radiation curves and the lack of deviation in the degree-day curves. Topographic heterogeneighty plays a large role in the magnitude of the improvement as indicated by comparing the curves in the Emerald and Topaz Lake Watersheds.

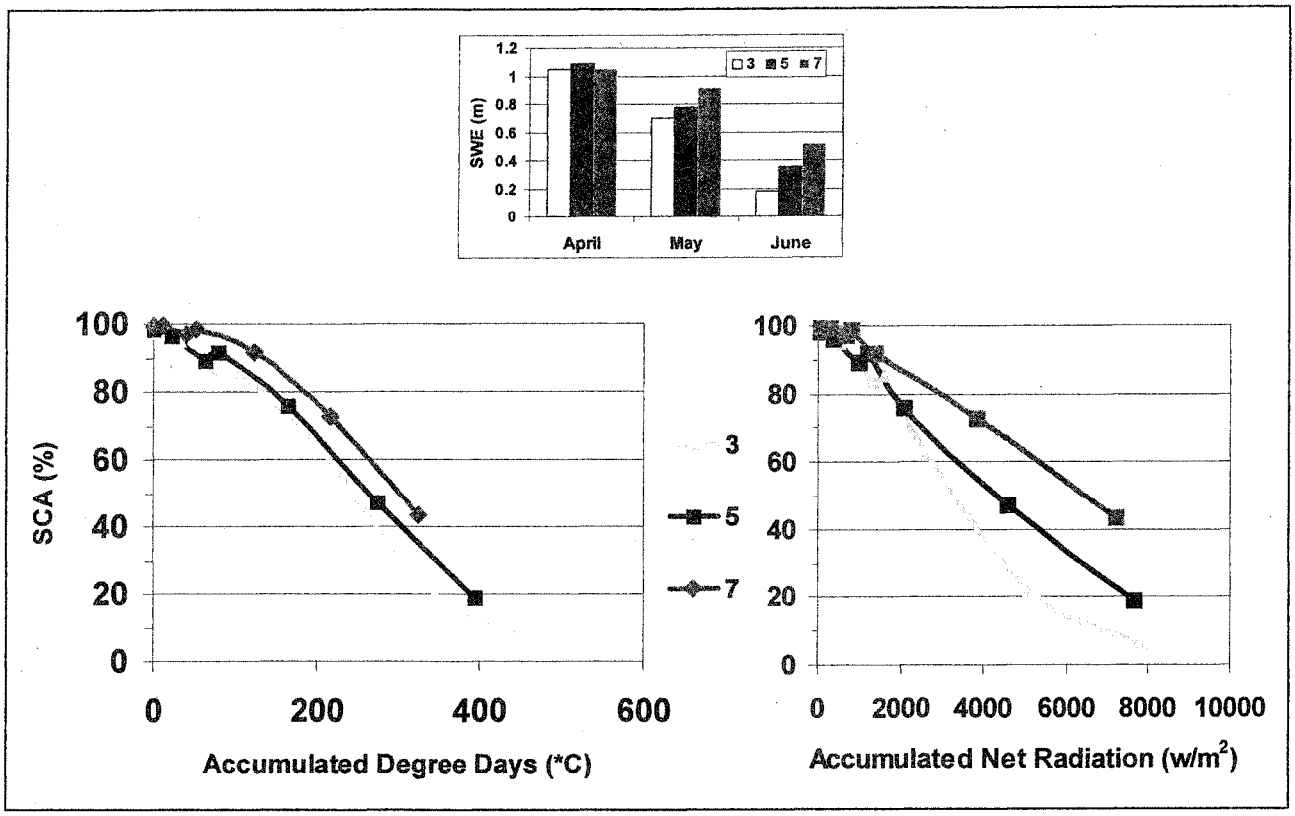

Figure 9: Accumulated degree-day and net radiation curves for elevation bands 3, 5 and 7 of the Tokopah Basin. SWE values for the three elevation bands are also shown.

FUTURE RESEARCH

In order to account for the thermal energy from one pixel to another, we would like to apply a terrain model to estimate incoming longwave radiation. Additionally we would like to incorporate remotely sensed albedo data into the net radiation model. Incorporating an analysis over multiple snowmelt seasons would also be useful in assessing the ability of the two methods to represent snow cover depletion. Lastly, we would like to improve our estimates of distributed SWE used to validate the curves by using binary regression trees as described by Elder et al. (1995).

ACKNOWLEDGEMENTS

Financial support was provided by NASA's EOS Interdisciplinary Investigation on "Hydrology, Hydrochemical Modeling, and Remote Sensing in Seasonally Snow-Covered Alpine Drainage Basins" and by the National Science Foundation's Center for the Sustainability of semi-Arid Hydrology and Riparian Areas (SAHRA). Stephen Fassnacht and Kevin Dressler provided comments and insight. The authors are particularly indebted to all of the individuals who participated in the data collection.

LITERATURE CITED

Cline, D. W., K. Elder, and R. C. Bales, Scale effects in a distributed snow water equivalence and snowmelt model for mountain basins, *Hydrological Processes*, 12 (10-11), 1527-1536, 1998a.

Cline, D. W., R.C. Bales, and J. Dozier, Estimating the spatial distribution of snow in mountain basins using remote sensing and energy balance modeling, *Water Resources Research*, 34 (5), 1275-1285, 1998b

Colee, M. T., 2000, A high-resolution distributed snowmelt model in an alpine catchment, M.A. Thesis, University of California at Santa Barbara.

Daly, C., R. P. Neilson, and D. L. Phillips, A statistical topographic model for mapping climatological precipitation over mountainous terrain, *Journal of Applied Meteorology*, 33 (2), 140-158, 1994.

Dozier, J., A clear-sky spectral solar radiation model for snow-covered mountainous terrain, *Water Resources Research*, 16, 709-718, 1980.

Dozier, J., and J. Frew, Rapid calculation of terrain parameters for radiation modeling from digital elevation data, IEEE Transactions on Geoscience and Remote Sensing, 28 (5), 963-969, 1990.

Dubayah, R., Using LOWTRAN7 and field flux measurements in an atmospheric and topographic solar radiation model, in Proceedings IGARSS '91, pp. 39-42, IEEE 91CH2971-0,1991.

Elder, K., Michaelsen, J., Dozier, J., Small basin modeling of snow water equivalence using binary regression tree methods, International Association of Hydrological Sciences, pp.129-139, Publication No.228: Great Yarmouth, 1995.

Idso, S. B., A set of equation for full spectrum and 8- to 14- um and 10.5- to 12.5-um thermal radiation from cloudless skies, Water Resources Research, 17 (2), 295-304, 1981.

Jordan, R., A one-dimensional temperature model for a snow cover, Special Report 91-6, US Army Cold Regions Research and Engineering Laboratory, Hanover, NH, 1991.

Kneizys, F. X.., E.P. Shettle, L. W. Abreu, J. H. Chetwynd, G. P. Anderson, W. O. Gallery, J.E. A. Selby, and S. A. Clough, User's Guide to LOWTRAN7, Report AFGL-TR-88-0177, Air Force Geophysics Laboratory, Bedford, MA, 1988.

Lillesand, T.M., and R.W. Kiefer, 1987, Remote Sensing and Image Interpretation, 2nd Edition, Wiley, NY.

Rango, A., and J. Martinec, Snow accumulation derived from modified depletion curves of snow coverage, *Hydrological Aspects of Alpine and High Mountain Areas* (Proceedings of the Exeter Symposium, July 1982). IAHS Publ. No. 138.

Raskin, R. G., C. C. Funk, and S. R. Webber, Spherekit, the spatial interpolation toolkit, Technical Report 97-4, NCGIA, Santa Barbara, CA, 1997.

Rosenthal, Walter and Jeff Dozier, Automated mapping of montane snow cover at subpixel resolution from the Landsat Thematic Mapper, *Water Resources Research*. Vol. 32, no.1, 115, January 1996.

Thornton, P. E., S. W. Running, and M. A. White, generating surfaces of daily meteorological variables over large regions of complex terrain, *Journal of Hydrology*, 190, 214-251, 1997.

Tonnessen, K. A., The Emerald Lake watershed study: introduction and site description, *Water Resources Research*, 27 (7), 1537-1539, 1991.

Willmott, C. J., and K. Matsuura, Smart interpolation of annually averaged air temperature in the United Sates, Journal of Applied Meteorology, 34 (12), 2577-2586, 1995.